RADIATION INDUCED SURFACE EFFECTS ON SELECTED SEMICONDUCTOR DEVICES

U. COCCA
and
N.B. KOEPP-BAKER

GENERAL ELECTRIC COMPANY

Presented at
ANS-ASTM Joint Conference on
Radiation Effects in Electronics
Syracuse, New York
October 1964

Myron C. Nagurney
NASA Evaluator
7/22/65

NASA CR # 63776

FACILITY FORM 602
N65-86039
(ACCESSION NUMBER)
40
(PAGES)
(NASA CR OR TMX OR AD NUMBER)
(THRU)
None
(CODE)
(CATEGORY)

Radiation Induced Surface Effects on
Selected Semiconductor Devices*

By U. Cocca[1] and N. B. Koepp-Baker[2]

Key Words - Co^{60} radiation, surface effects, semiconductor, bulk damage, space radiation, transistors, diodes, zener diodes, field effect transistors, permanent damage, recovery, annealing, radiation effects, Nimbus.

Abstract - A preliminary investigation into the effects of space indigenous radiation on a number of semiconductor devices is described. A Co^{60} source was used to irradiate the devices to an ionization level equivalent to that received by a satellite in a typical orbit in a six-month period. Transistor I_{CBO} and diode I_R were monitored throughout the irradiation and pre-test and post-test transistor gain measurements were made. The results of the irradiation test are presented in graphical and tabular form. In general, transistor and diode reverse current increased and transistor gain decreased during irradiation. Some recovery was evidenced following storage and temperature annealing cycles.

Introduction

The damage induced in semiconductor devices subjected to a radiation environment, such as that encountered by a satellite, is of sufficient magnitude that degradation of the electrical characteristics of these devices must be considered in the design of any satellite. The effects of radiation on semiconductors are classified as surface or bulk effects, depending upon the damage mechanism involved. Bulk effects arise from the production of electron-hole pairs in the semiconductor crystal by ionizing radiation, and from the production of defects in the crystal lattice by high energy particles. Although surface effects are not clearly understood, it is theorized that they arise from the ionization of the encapsulating gas and the interaction of this ionized gas with the surface of the semiconductor material. Surface effects are the predominant damage mechanism at lower radiation exposures and hence are the effects of particular interest. Neither the exposure rate nor the type of radiation appears to be significant, but rather the total amount of ionization produced has been found to be the controlling factor. This conclusion permits the use of gamma radiation to simulate the surface effects which would be produced by the radiation received in space, although space radiation consists predominantly of protons and electrons (1) (2).

The objective of this test was to determine the relative sensitivities of particular semi-conductor devices to ionizing radiation and the magnitude of the radiation effects problem existing in the Nimbus environment. It has been determined by prior experimentation that the

parameter particularly sensitive to surface effects in the majority of device types is the collector to base leakage current (I_{CBO}) for transistors and reverse leakage current (I_R), for diodes. Hence, these parameters were monitored during the irradiation to determine the sensitivity of the devices. The radiation-induced surface effects on transistor gain were determined, separating the surface effects from the bulk effects. The degree of surface damage is dependent upon the collector bias and the electric potential existing in the transistor can, the effects of which are not fully understood. In addition, the radiation-induced surface effects exhibit recovery and memory phenomena. Recovery is evidenced on removal of bias, radiation, or both, although the respective rates are different. Memory is experienced on re-irradiation; that is, a device will tend to reach its previously damaged state at a considerably lower radiation exposure. However, memory phenomenon can be erased and the initial I_{CBO} characteristics completely restored by annealing at elevated temperatures.

Irradiation Experiment

A Co^{60} gamma radiation source was utilized to perform the irradiation tests. The activity of the source was approximately six thousand curies producing a maximum dose rate of 10^5 Roentgens per hour at the sample location. The ambient temperature varied between 25C and 31C during the test.

The devices tested consisted of samples of each available type of transistor and diode listed on the approved Nimbus parts list and considered to present a potential surface effects problem. Table 1 lists the devices

tested, noting such pertinent information as: type, class, structure, material, and number tested. In addition, the column titled "Case Connection", notes which lead (emitter, base, or collector) is in electrical contact with the case, as this affects the electric field inside the transistor can and hence influences the magnitude of the surface effect.

The intense radiation close to the Cobalt source precludes measurement of I_{CBO} in a normal manner; therefore, all monitoring was performed remotely. I_{CBO} and I_R were measured by monitoring the voltage developed across a resistor inserted in series with the appropriate junction. Schematics of the test circuits are presented in Figure 1. The schematics do not show all the components tested; one of each type is depicted and is representative of all units of its type. The collector-base junction of each transistor is reverse biased at ten volts. A 10-volt bias was selected as it appears to be the bias potential at which surface effects are generally more pronounced. The signal diodes were reverse biased at the same potential.

The circuit used to test the Zener diodes appears in Figure 1. A load resistor is required to operate the Zener diode at its rated current, and the Zener voltage is monitored through a voltage divider. All components were mounted on phenolic boards and encapsulated in Dow Silguard #182 to eliminate the effects of air ionization. The voltage drops across the monitoring resistors were measured by a digital voltmeter, and the values were automatically recorded by an electronic printer. In addition to the tests mentioned above, the collector characteristic curves of five selected

transistor types were monitored during irradiation. The collector-base junctions of these transistors were reverse biased at nine volts, except for brief periods during which the collector characteristics were monitored.

Pre-test measurements were made on all components prior to irradiation. The components were then mounted and connected to the measuring equipment through 40 feet of shielded cable. Measurements were made at different exposures, a synopsis of which appears in Figure 2. Initially, the irradiation source was removed during the measurement period to eliminate spurious ionization currents. However, after several measurement periods, the spurious currents were determined to be less than the sensitivity of the current measuring circuit (10^{-9} amps) and measurements were then recorded with the devices in the gamma source environment. All components were irradiated to a total exposure of approximately 10^7 Roentgens. The bias supply voltages were monitored throughout the test and these voltages remained within 2 percent of their nominal values. Post-test measurements, including collector characteristics and I_{CBO} values, were made four weeks after irradiation. All the transistors were subsequently heated at 95C for two hours, and the post-test measurements were repeated to determine the annealing characteristics and to estimate the amount of damage contributable to bulk effects. Throughout this report the four-week time period mentioned above will be referred to as post or storage, and the heat treatment will be referred to as annealing.

Results and Discussion

The radiation induced damage to the devices resulting from the gamma irradiation is depicted in Figures 3 through 22. The recovery from the induced damage is shown in Tables 2 and 3. The average values shown in Figures 3 through 16 are presented in lieu of a better method, and use of these averages should be limited accordingly. The ratios of average values summarized in Tables 2 and 3 are calculated by deleting any values not in agreement with the bulk of the data recorded for these devices. These "weighted" averages and average values are used solely for convenience but could be utilized for device selection, taking into account the extreme range of values for a given device type.

The results of the irradiation test revealed specific information which may not be readily evident from the graphs and tables presented. The following discussion will attempt to enlighten these results.

Diode Test Results

Two types of signal diodes and two types of Zener diodes were tested. The Zener diodes (types 1N758A and 1N821) exhibited no change in reference voltage (measured at rated current) at an exposure of 10^7 Roentgens. The reverse leakage current of the type 1N914 diodes remained unaffected by a radiation exposure of 10^7 Roentgens (Figure 3). Pre- and post-test reverse breakdown characteristics are presented in Figure 17a and b, respectively. No change in breakdown voltage is apparent. Two type MQ-1 diodes were tested. Each unit contains four individual diodes and the results are presented as if eight single units were tested. The reverse leakage current of the MQ-1 diodes increased by one to two orders of magnitude during an exposure of 10^7 Roentgens (Figure 4). However,

the leakage current recovered to approximately its pre-test value during a four-week storage period (Table 2). Typical pre- and post-test reverse breakdown characteristics are presented in Figure 17c and d, respectively. Three of the eight units tested exhibited a change in breakdown characteristics. The pre- and post-test characteristics of one device which exhibited this breakdown phenomenon are presented in Figure 17e and f, respectively. The change in breakdown characteristics is indicated by the double break in the knee of the curve in Figure 17f, and can be associated with microplasma phenomenon, indicating that the radiation damage may be manifested as inhomogeneities at the junction depletion region.

Transistor Test Results

To facilitate discussion, the results of the transistors tested are grouped by material and structure.

Germanium Transistors (Types 2N396A and 2N1358A) -- Both units tested are p-n-p, alloy structure devices and both exhibited a twofold increase in I_{CBO} after an exposure of 10^7 Roentgens (r) (Figures 5 and 12). This increase in I_{CBO} persisted during storage and was removed by annealing (Table 3). The radiation-induced changes in gain characteristics are less well behaved. The type 2N1358A transistors showed no apparent surface effect on gain characteristics, as the degradation observed was no greater than the predicted bulk damage. The type 2N396A transistors responded in the opposite manner; that is, the gain degradation was greater than is explainable by bulk damage alone. In addition, when these units were subjected to an annealing cycle, no gain recovery was evidenced. Figure 18

presents the variation in gain as a function of radiation for the type 2N396A transistor. This graph represents a sample size of one and is not necessarily representative of the group tested. The apparent increase in gain can be explained by noting the increase in I_{CEO}.

Silicon Transistor Alloy Junction (Type 2N1676) - - The test results on this type of transistor are somewhat contradictory in that some of the units possessed improved characteristics after irradiation. The improved characteristics are brought about by a complex surface interaction produced by radiation-induced ionization. In spite of the confusing nature of the recovery and annealing data, it is important to note that the I_{CBO} of this type of transistor increased by four orders of magnitude during irradiation (Figure 14). The variations in the current gains, however, are well behaved. The gains decreased during the test and recovered during storage and annealing to a final degraded value consistent with bulk damage estimates (Table 3).

Silicon Transistor Diffused Junction (Type 2N1248) - - The observed degradation of current gain and leakage current characteristics of the type 2N1248 transistor is typical of radiation-induced surface effects. I_{CBO} increases three orders of magnitude during irradiation (Figure 11) and subsequently decreases during storage and annealing to a value consistent with the bulk damage predictions (Table 3). The current gain data is in agreement as, during irradiation, these parameters have degraded and some recovery is evidenced following an annealing cycle.

Silicon Transistor Mesa (Type 2N1132) - - The test results from these units are contradictory enough to demand further investigation. The large increases in I_{CBO} (Figure 10) should be noted, but the discrepancy between the characteristics after annealing and the predicted bulk damage precludes any general comment on this device. The gain degradation during irradiation of a single unit is depicted graphically in Figure 19.

Silicon Transistors Planar (Types 2N657, 2N697, 2N708, 2N930, 2N1613, 2N2060 and 2N2604) Figures 6 to 9, 13, 15, 16, respectively - - With the exception of a few individual devices and the types 2N708 and 2N2604, the observed variations in I_{CBO} are similar. During irradiation, I_{CBO} increases from two to four orders of magnitude, with the I_{CBO} of the majority of devices increasing three orders of magnitude. During storage the respective I_{CBO} recovers to within an order of magnitude of its original value. A subsequent annealing cycle produces a further recovery, which, considering bulk damage effects, essentially returns I_{CBO} to its initial value (Table 3). The two types of planar devices which exhibited different characteristics are basically different devices. The type 2N708 transistor is a silicon, n-p-n device similar to the others in this group with the exception that this device has a much higher alpha cut-off frequency ($f_{\alpha b}$). These units did not exhibit the usual I_{CBO} increase. This result may be explainable by considering the doping profile and the thicker passivation layer at the base-collector region of the device, thus providing more resistance to channel formation. The type 2N2604 transistor is a p-n-p device, and as might be expected, exhibits different channeling

characteristics. The I_{CBO} of these units increased three orders of magnitude during irradiation, and subsequent storing and annealing did not improve this characteristic appreciably. The changes in gain characteristics of all the planar units tested were similar. However, the gain decreased to a value lower than that predicted for bulk damage. This large decrease in gain did not fully recover during storage or annealing. The gain degradation as a function of radiation exposure is depicted for single units of types 2N697 and 2N1613 in Figures 20 and 21, respectively. The degradation and partial recovery of a type 2N708 transistor is depicted in Figure 22. The gain degradations and particularly the non-linear beta at low base currents, imply that base to emitter surface channels were formed.

Conclusions

The radiation-induced surface effects in transistor and diode structures are extremely complex phenomena. The purpose of this test was to determine the magnitude of the radiation-induced surface effects of a selected group of transistors and diodes in a specified environment. No attempt was made to test a statistically meaningful number of each type of component, nor was a selection procedure utilized to assure that those devices tested were not a biased sample. Although conclusions, in the strict definition, cannot be drawn from the test results, a number of guidelines or hypotheses can be noted. These guidelines are noted in the following paragraphs for devices irradiated to 10^7 Roentgens.

The surface effects problem in diodes is less severe than in other semiconductor devices due in part to the absence of an electric field such as that produced between the metal can and the pellet of a typical transistor. Also, since the diode has only one p-n junction, the surface effects are not as complex as those existing in a two-junction device. The Zener diodes exhibited no change in breakdown voltage at rated current, and, when utilized at rated currents, surface effects should represent no problem. However, if Zener devices are to be utilized at low currents, surface effects may become significant.

The circuitry utilized to test the transistors did not employ the transistors in the usual manner; the results, therefore, are not directly related to the changes that would occur in characteristic transistor circuitry. However, the following statements regarding the transistors tested are offered to assist the designer in selecting the most resistant components. The germanium units exhibited minimum changes in I_{CBO}. Whether this is attributable to the fact that the units are germanium or that the radiation-induced changes are negligible, in comparison with the initial I_{CBO} values, is not known. If the circuit design is such that a 50 percent gain degradation is allowable, these units should perform the desired function. The silicon units present such a wide variety of results that each unit should be treated individually. The type 2N1676 units exhibited

large I_{CBO} increases (10^4) but relatively small gain degradations. The 2N1248 units exhibited I_{CBO} increases of two orders of magnitude and large gain degradations. The 2N1132 units are degraded beyond normal usefulness, exhibiting I_{CBO} increases of greater than 10^5 and gain degradations of greater than 70 percent. The low-frequency planar units were similar and exhibited I_{CBO} increases of two to four orders of magnitude and gain degradations of 80 to 95 percent. The 2N708 exhibited no I_{CBO} increase but gain degradations of 80 percent were observed. The type 2N2604 exhibited large I_{CBO} and gain changes. The type 2N2060 is a dual unit, and it should be noted that the changes in parameters of the two adjacent units in each can were approximately identical.

Footnotes

*Work supported by NASA under contract NAS-5-1347.

[1]Radio Guidance Operation, General Electric Co., Syracuse, N.Y.

[2]Radiation Effects Operation, General Electric Co., Oklahoma City, Oklahoma.

(1) R. R. Blair, "Surface Effects of Radiation on Transistors", IEEE, Transactions on Nuclear Science, Vol NS-10, No.5, Nov. '63 pp 35 - 44 .

(2) H. A. Zagorites, et al, "Some Effects of Transit Gamma Radiation on Transistors", IEEE, Transactions on Nuclear Science, Vol NS-10, No. 5, Nov. '63, pp 45 - 53.

Table 1 -- Components Tested

Type	Class	No. Tested	Material	Structure	Case Connection	Use	f_t min, Mc
2N396A	p-n-p	6	Ge	Alloy	Base	Low level switch	5[a]
2N657	n-p-n	5	Si	Planar	Collector	Power	70
2N697	n-p-n	6	Si	Planar	Collector	High frequency switch	70
2N708	n-p-n	6	Si	Planar	Collector	Hi speed switch	300
2N930	n-p-n	5	Si	Planar	Collector	Small signal-low noise	30
2N1132	p-n-p	6	Si	Mesa	Collector	Power switch	60
2N1246	n-p-n	5	Si	Diffused Junc.	Isolated	Low noise	5[a]
2N1358A	p-n-p	5	Ge	Alloy	Collector	Power switch	5[b]
2N1613	n-p-n	6	Si	Planar	Collector	General purpose	60
2N1676	p-n-p	5	Si	Alloy	Collector	Low level chopper	40[a]
2N2060	n-p-n	5	Si	Planar Dual	Isolated	Differential amp.	60
2N2604	p-n-p	5	Si	Planar	Collector	Low level-high gain	30
1N750A	Zener	5	Si	...	...	Voltage regulator	...
1N821	Zener	5	Si	...	...	Voltage reference (temp. comp.)	...
1N914	...	5	Si	...	...	Computer switch	...
MQ1	Matched	2	Si	Planar Epit. Pass....		Computer	...

[a] $f_{\alpha b}$ [b] $f_{\alpha e}$, kc

Table 2 -- Summary of Diode Damage and Recovery

Results are presented as ratios; i.e., value at time noted by column heading/ initial value.

Diode Type	Ratio of I_R at V_R = 10v	
	10^7r	Stored
MQ-1	40	1.3
1N914	1.0	1.0

Table . -- Summary of Transistor Damage and Recovery

Results are presented as ratios; i.e., value at time noted by column heading/initial value.

Transistor Type	Ratio of I_{CBO} at V_{CB} = 10v				Ratio of Gain at V_{CE} = 5v, I_B = 5ua				
					Stored		Annealed		
	$10^7 r$	Stored	Annealed	Note[a]	h_{fe}	H_{FE}	h_{fe}	H_{FE}	Note[a]
2N396A	2	2	1	...	.4	.6	...	.5	1
2N657	4×10^2	10	3	...	.1	.1	.3	.2	2
2N697	10^3	15	2	3	.1	.1	.3	.3	1
2N708	1	1	1	...	.2	.2	.4	.3	2
2N930	10^4	57	11	4	.05	.03	.1	.1	2
2N1132	2×10^4	5×10^4	10^2	5	.3	.3	.5	.5	1
2N1248	3×10^2	10	5	...	.07	.03	.1	.1	6
2N1554	2	2	1	...	.5	.5	...	.5	6
2N1613	3×10^3	50	2	...	.2	.1	.5	.4	2
2N1676	2×10^4	...	...	7	.6	.9	.7	.9	6
2N2060	10^2	10	3	8	.2	.1	.3	.2	2
2N2604	5×10^3	10^3	10^3	...	.2	.2	.2	.3	2

[a]Notes

1. Gain degradation greater than predicted bulk damage.
2. Damage about 50 percent greater than predicted bulk damage.
3. Ratio of four transistors; one did not recover but did anneal.
4. Ratio of four units; one unit exhibited much greater damage.
5. Large variation in recovery and annealing data.
6. Gain degradation in agreement with bulk damage estimate.
7. Degree of recovery unpredictable with some unit improving.
8. Average derived from 4 of 5 dual units; one dual unit exhibited much greater damage.

Illustrations and Captions

Figure 1 -- Test Circuit Schematics

Figure 2 -- Synopsis of Test Exposures

Figure 3 -- Radiation-Induced Damage (Diode Type 1N914)

Figure 4 -- Radiation-Induced Damage (Diode Type MQ-1)

Figure 5 -- Radiation-Induced Damage (Transistor Type 2N396A)

Figure 6 -- Radiation-Induced Damage (Transistor Type 2N657)

Figure 7 -- Radiation-Induced Damage (Transistor Type 2N697)

Figure 8 -- Radiation-Induced Damage (Transistor Type 2N708)

Figure 9 -- Radiation-Induced Damage (Transistor Type 2N930)

Figure 10 -- Radiation-Induced Damage (Transistor Type 2N1132)

Figure 11 -- Radiation-Induced Damage (Transistor Type 2N1248)

Figure 12 -- Radiation-Induced Damage (Transistor Type 2N1358A)

Figure 13 -- Radiation-Induced Damage (Transistor Type 2N1613)

Figure 14 -- Radiation-Induced Damage (Transistor Type 2N1676)

Figure 15 -- Radiation-Induced Damage (Transistor Type 2N2060)

Figure 16 -- Radiation-Induced Damage (Transistor Type 2N2604)

Figure 17 -- Reverse Characteristics of the 1N914 and MQ-1 Diodes

Figure 18 -- Radiation-Induced Gain Degradation (Transistor Type 2N396A)

Figure 19 -- Radiation-Induced Gain Degradation (Transistor Type 2N1132)

Figure 20 -- Radiation-Induced Gain Degradation (Transistor Type 2N697)

Figure 21 -- Radiation-Induced Gain Degradation (Transistor Type 2N1613)

Figure 22 -- Radiation Damage to Collector Characteristics (Transistor Type 2N708)

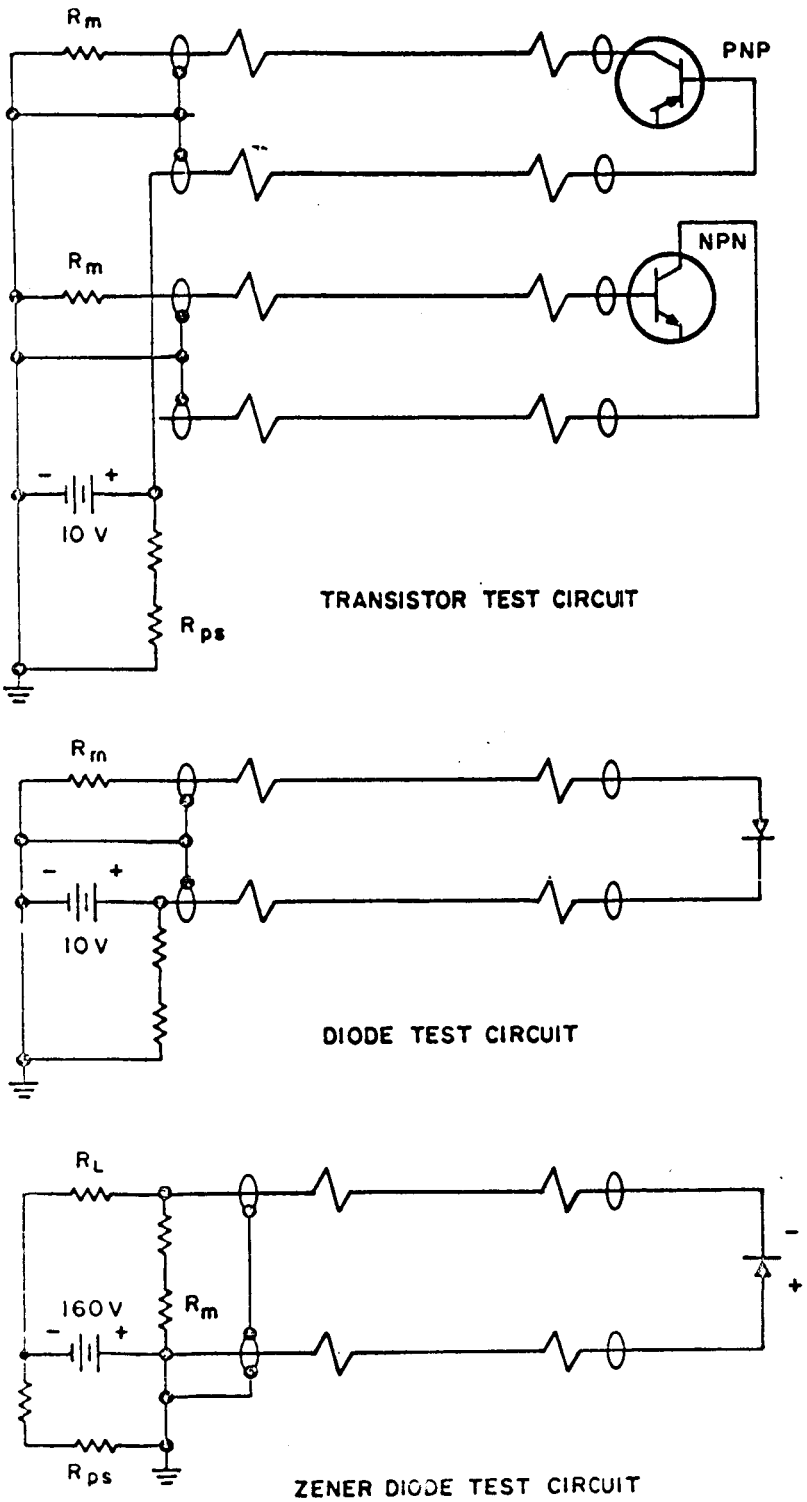

NOTE:
ALL INTERCONNECTING CABLES 40' OF NO. 22 AWG SHIELDED WIRE.

R_m = MONITORING RESISTOR

R_{ps} = POWER SUPPLY MONITORING RESISTOR

R_L = LOAD RESISTOR

Figure 1--Test Circuit Schematics

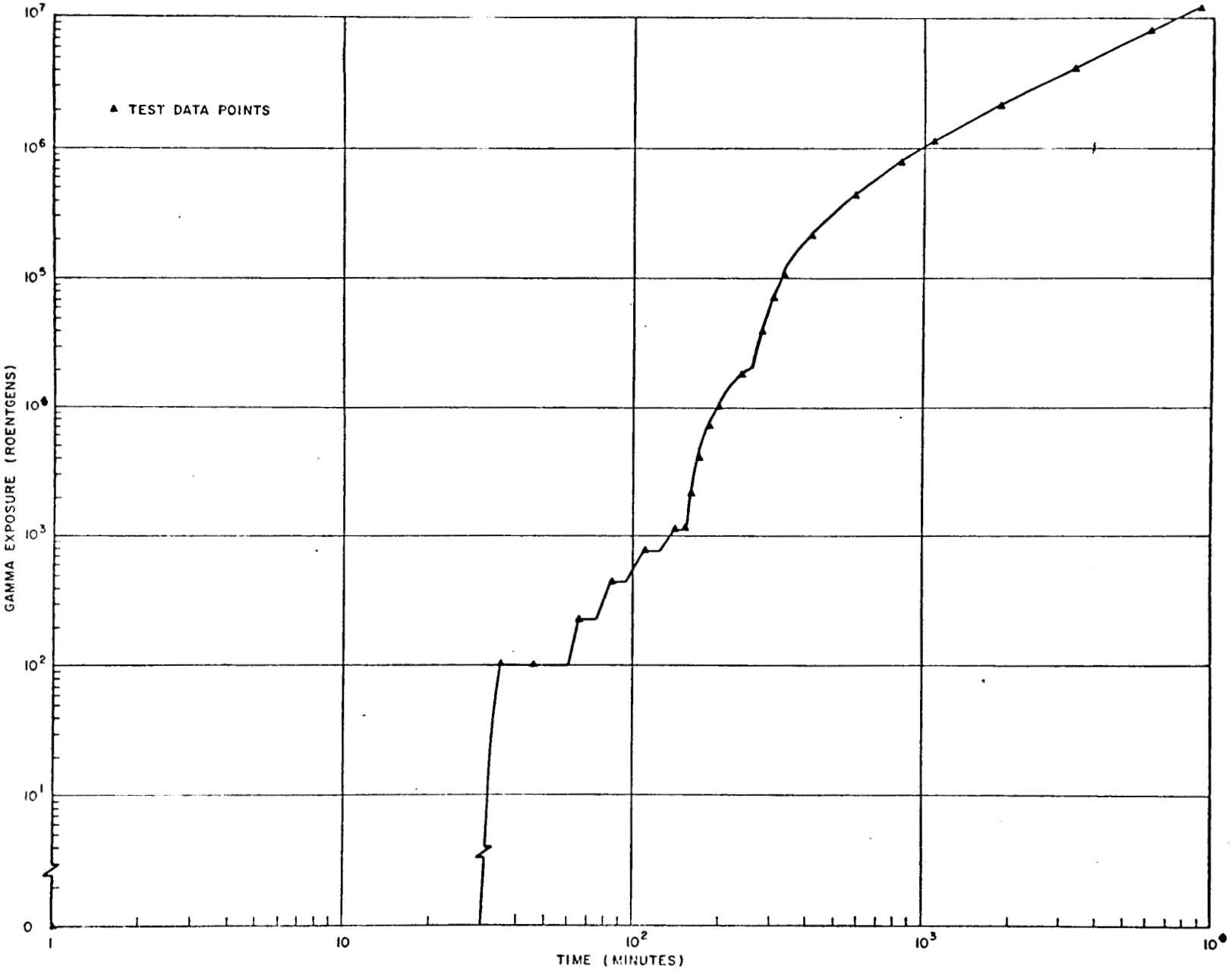

Figure 2--Synopsis of Test Exposures

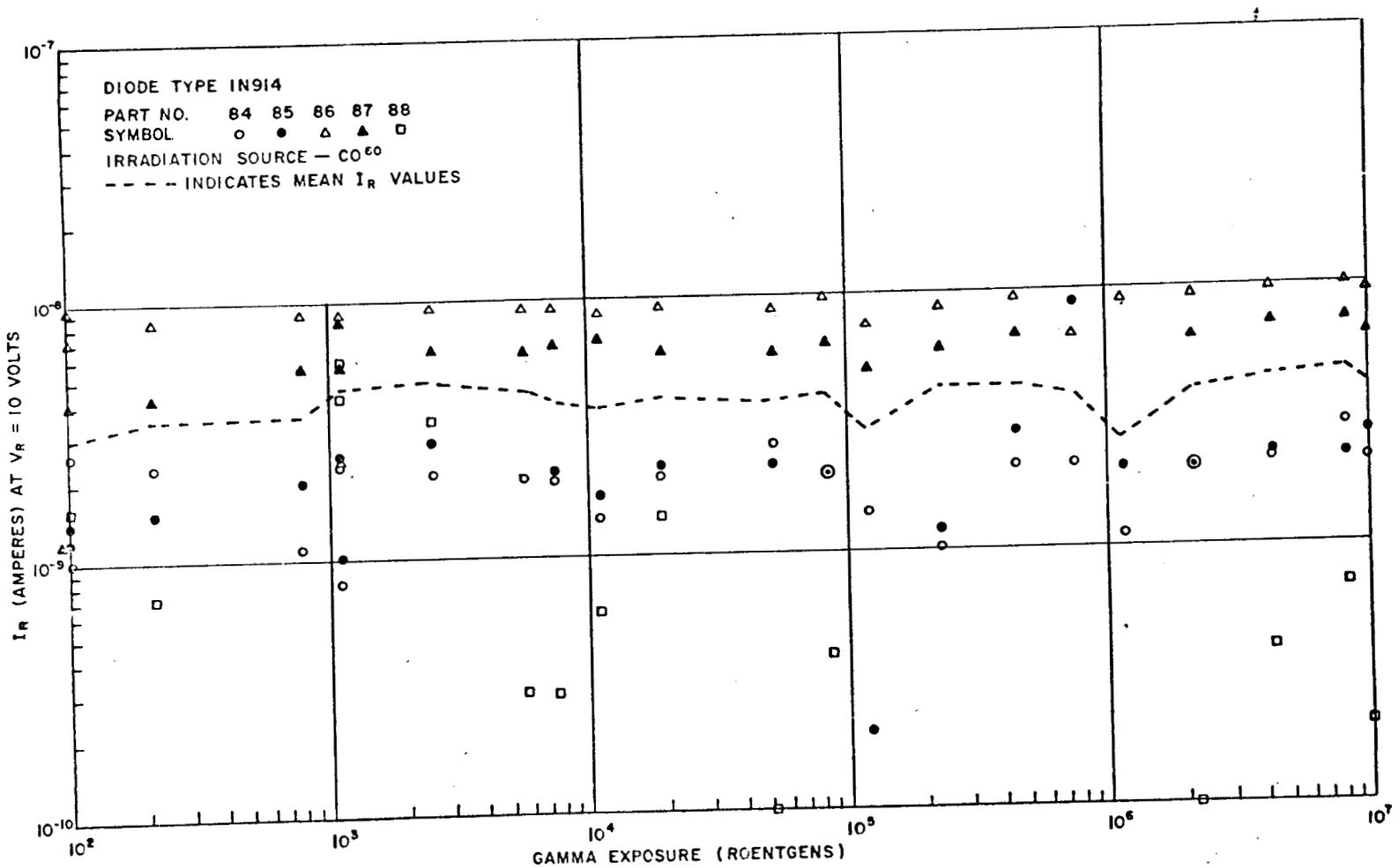

Figure 3-- Radiation-Induced Damage (Diode Type 1N914)

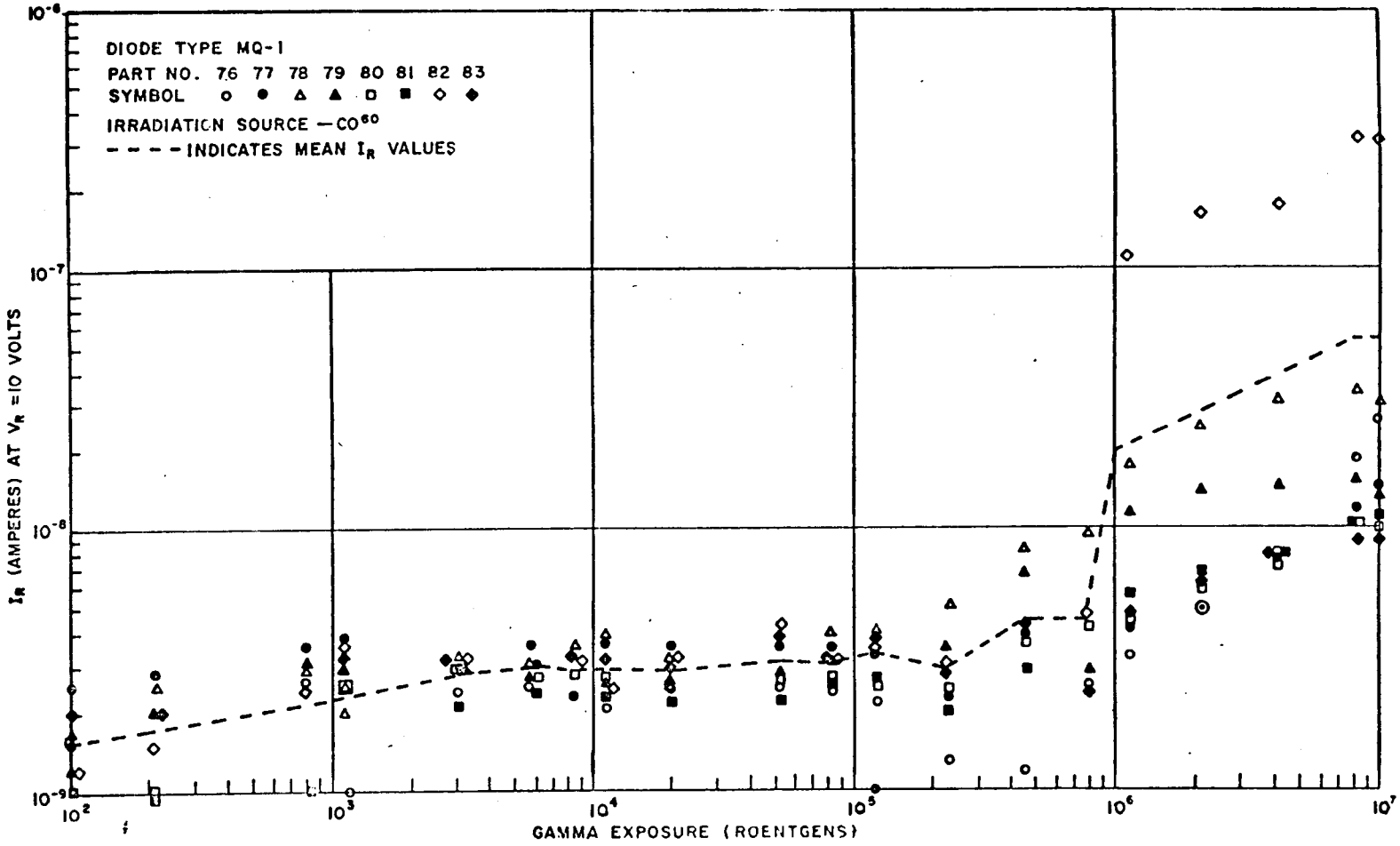

Figure 4 --Radiation-Induced Damage (Diode Type MQ-1)

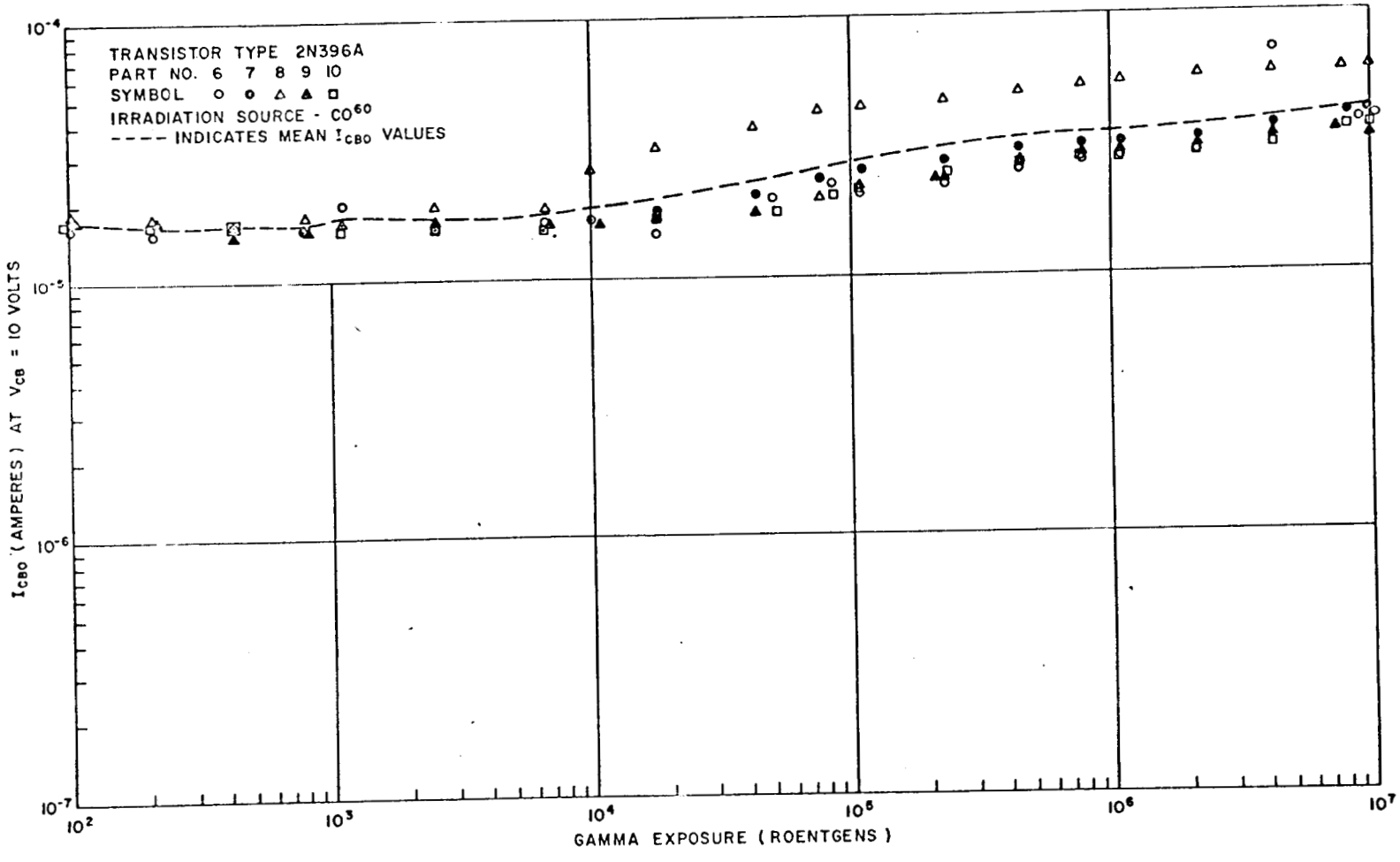

Figure 5-- Radiation-Induced Damage (Transistor Type 2N396A)

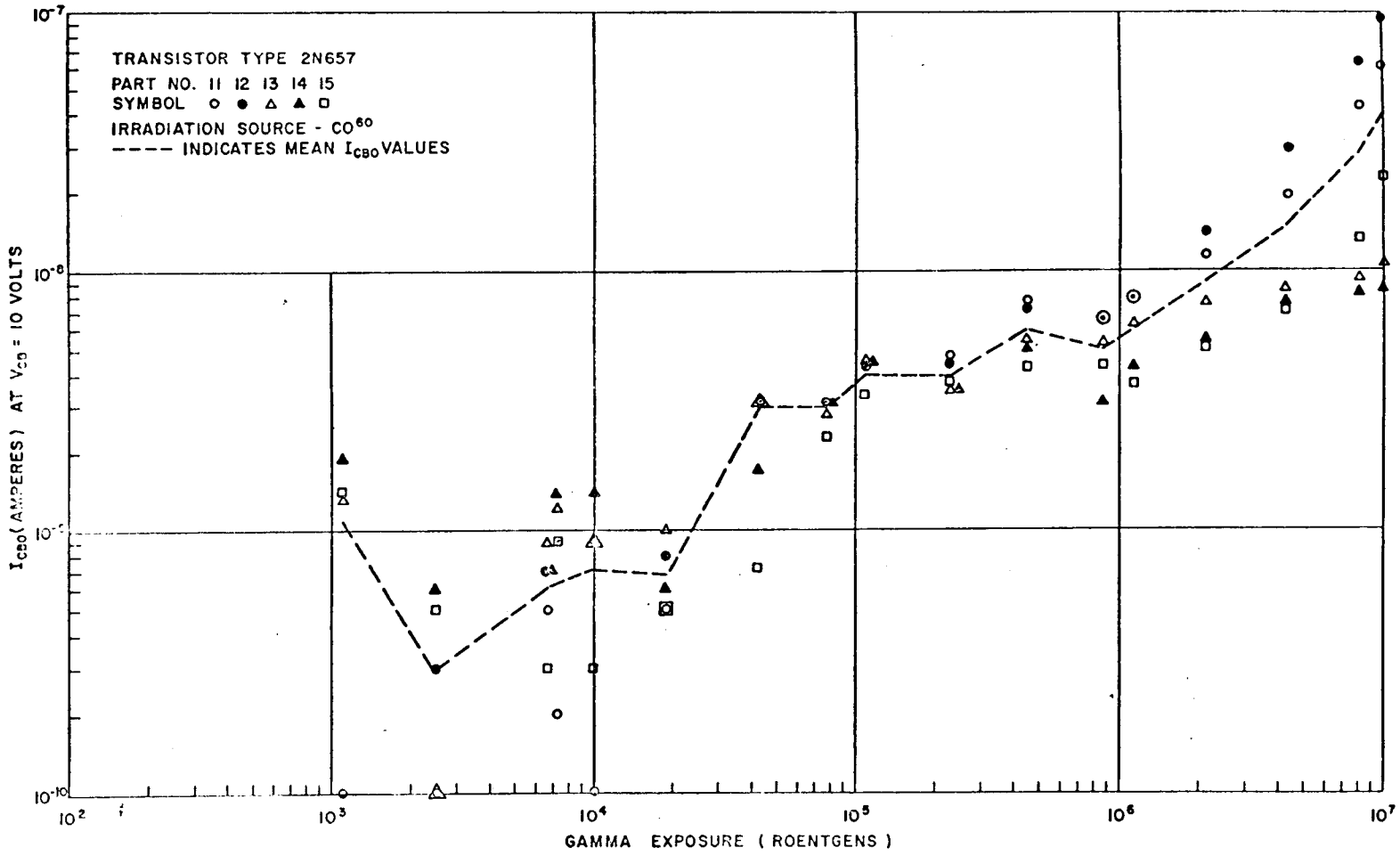

Figure 6--Radiation-Induced Damage (Transistor Type 2N657)

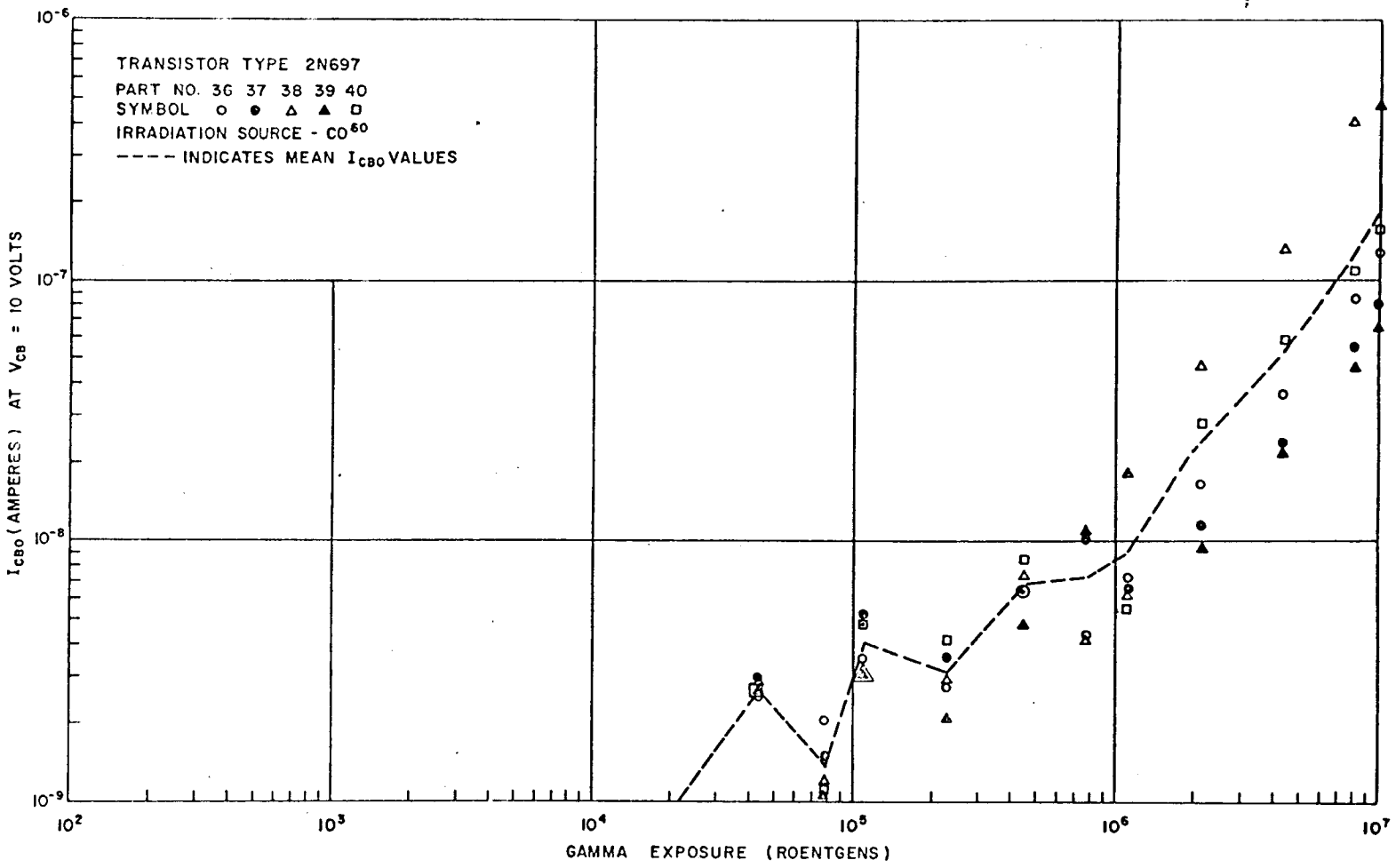

Figure 7 -- Radiation-Induced Damage (Transistor Type 2N697)

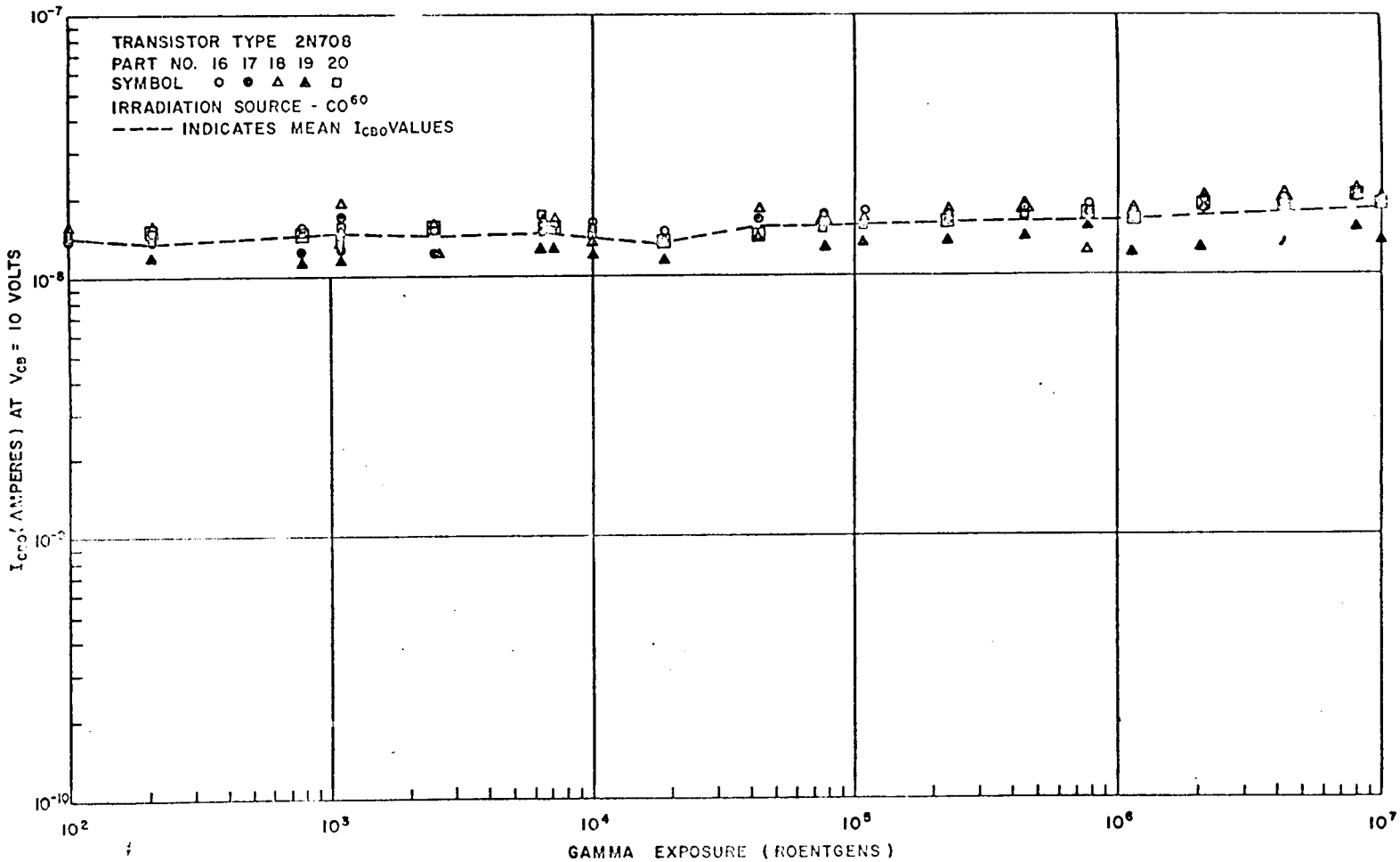

Figure 8--Radiation-Induced Damage (Transistor Type 2N708)

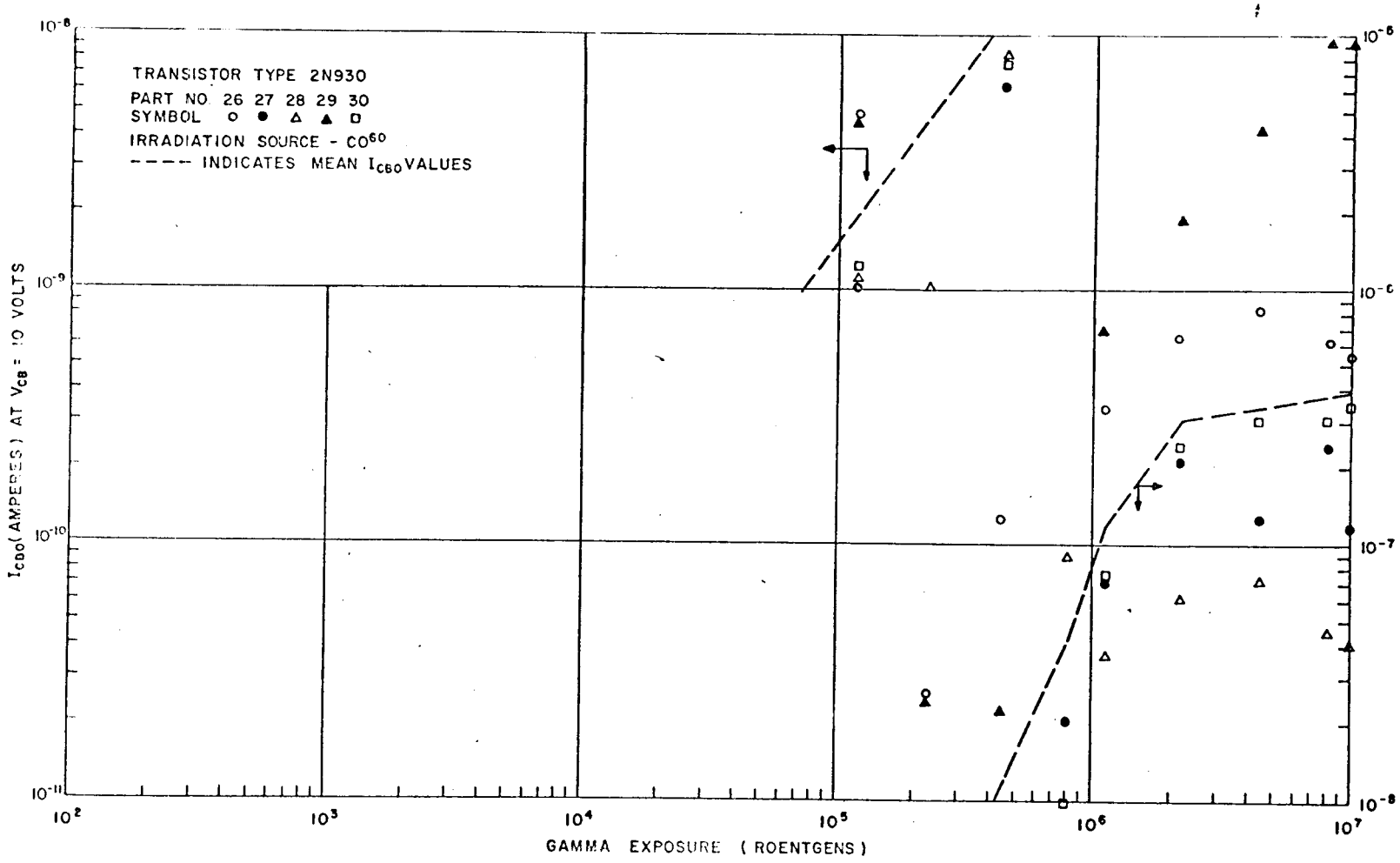

Figure 9 --Radiation-Induced Damage (Transistor Type 2N930)

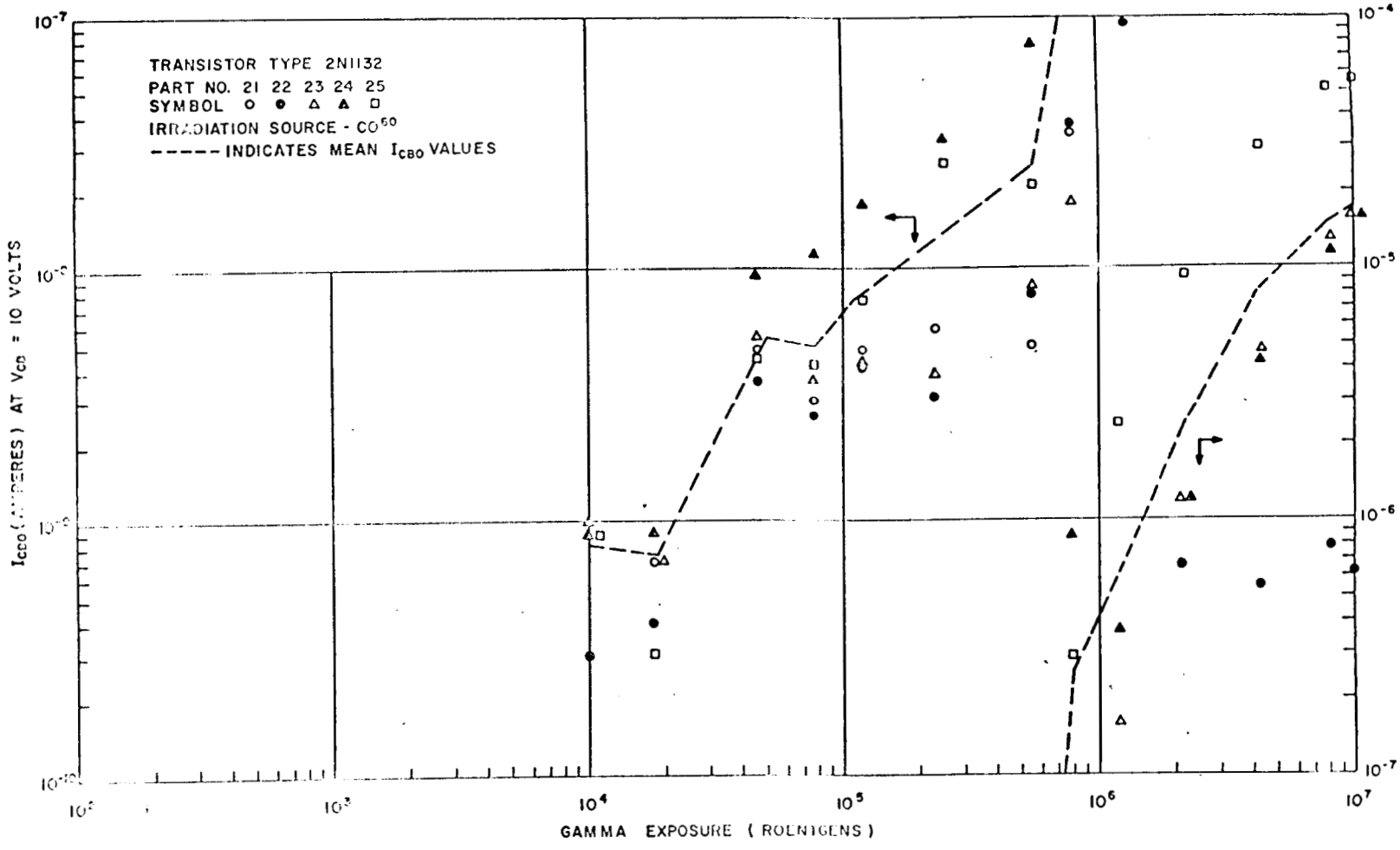

Figure 10--Radiation-Induced Damage (Transistor Type 2N1132)

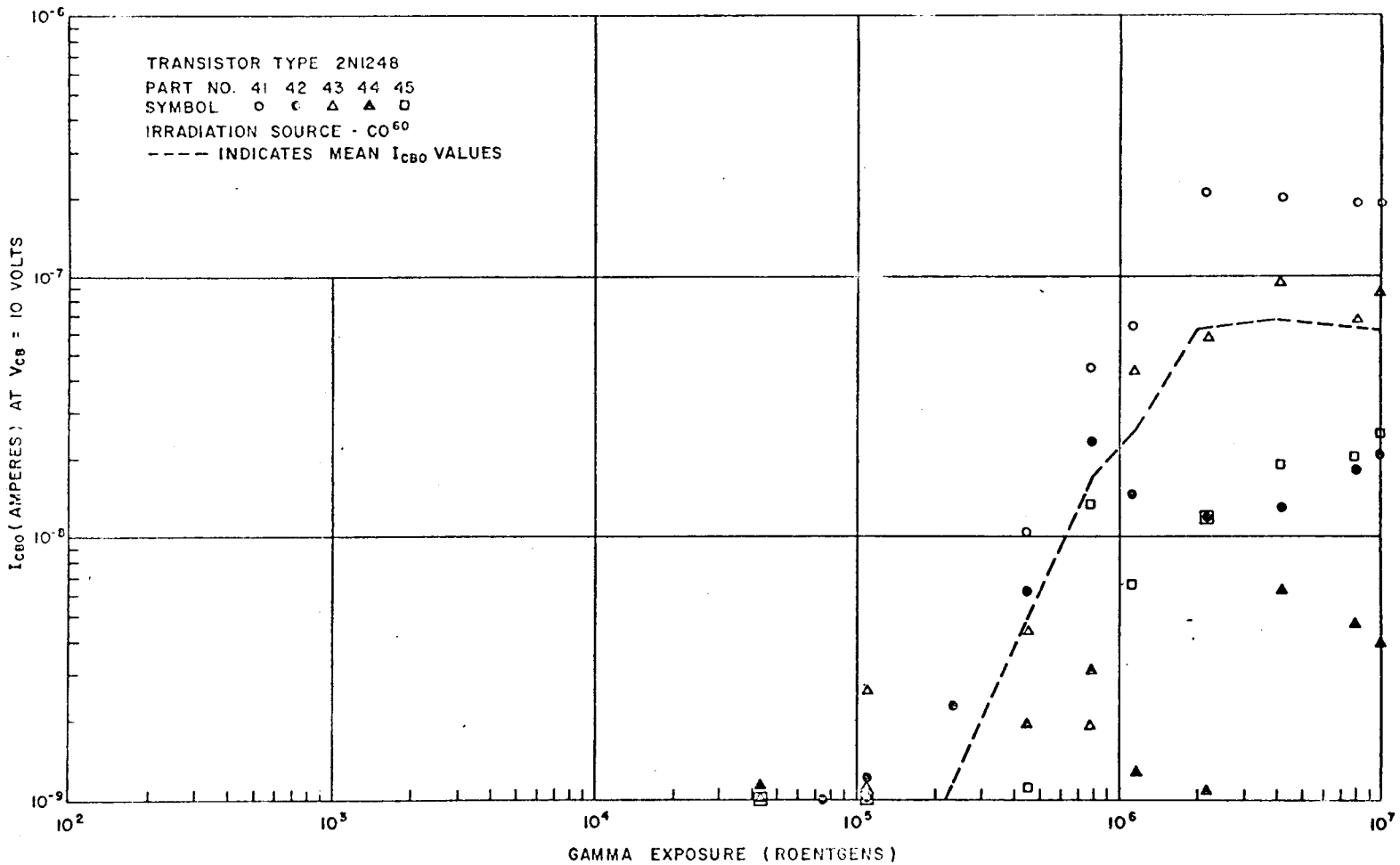

Figure 11 - Radiation-Induced Damage (Transistor Type 2N1248)

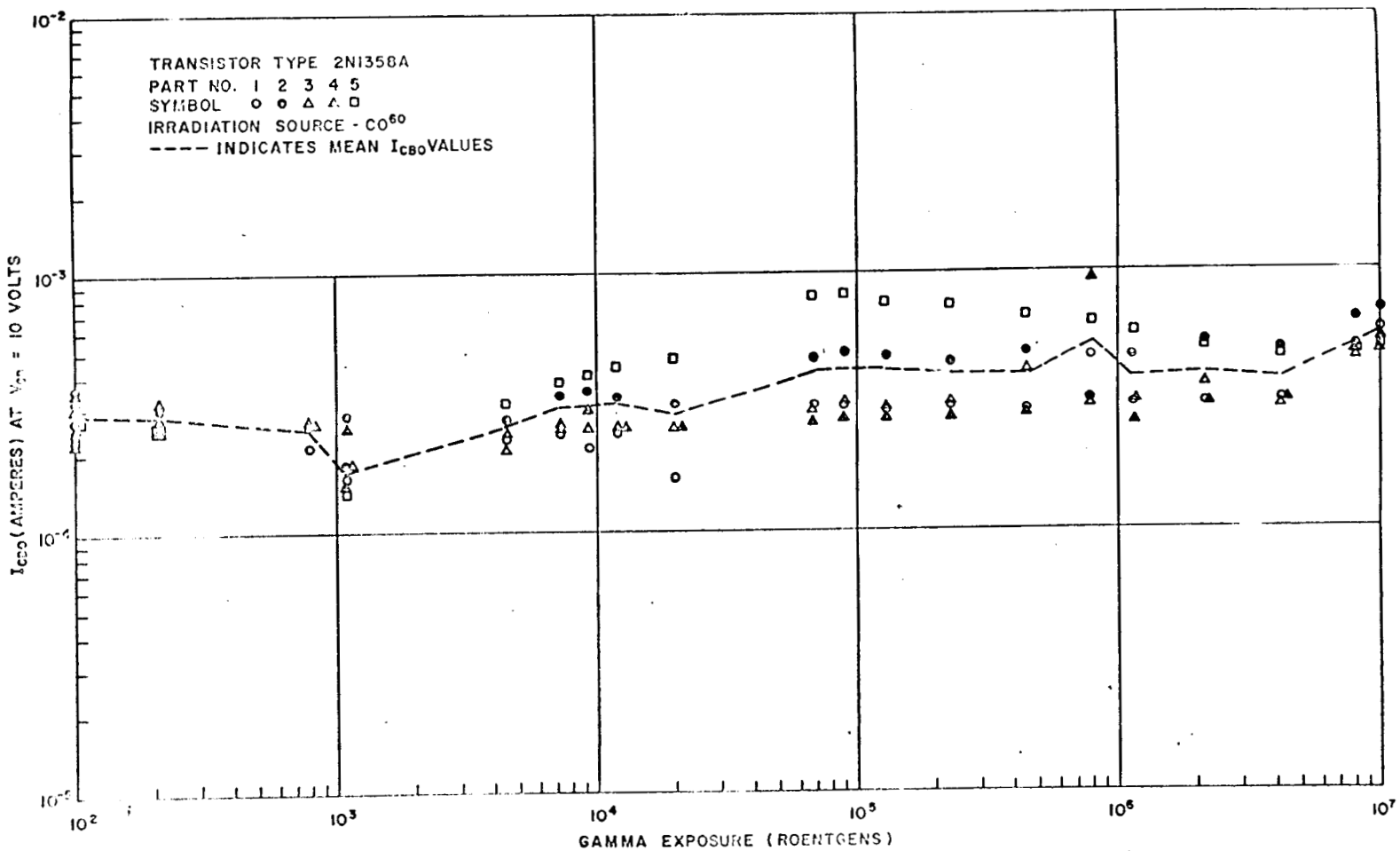

Figure 12 --Radiation-Induced Damage (Transistor Type 2N1358A)

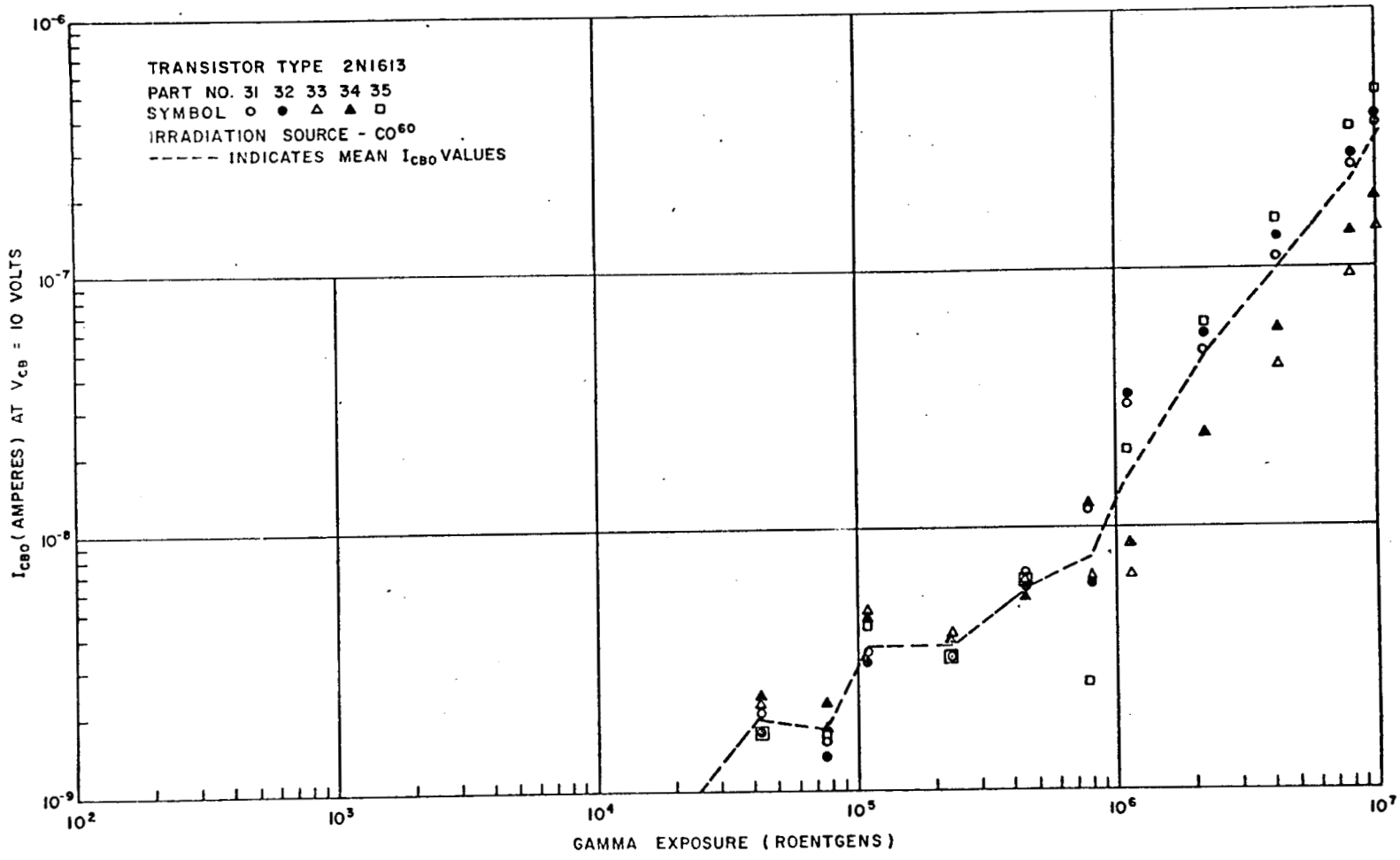

Figure 13--Radiation-Induced Damage (Transistor Type 2N1613)

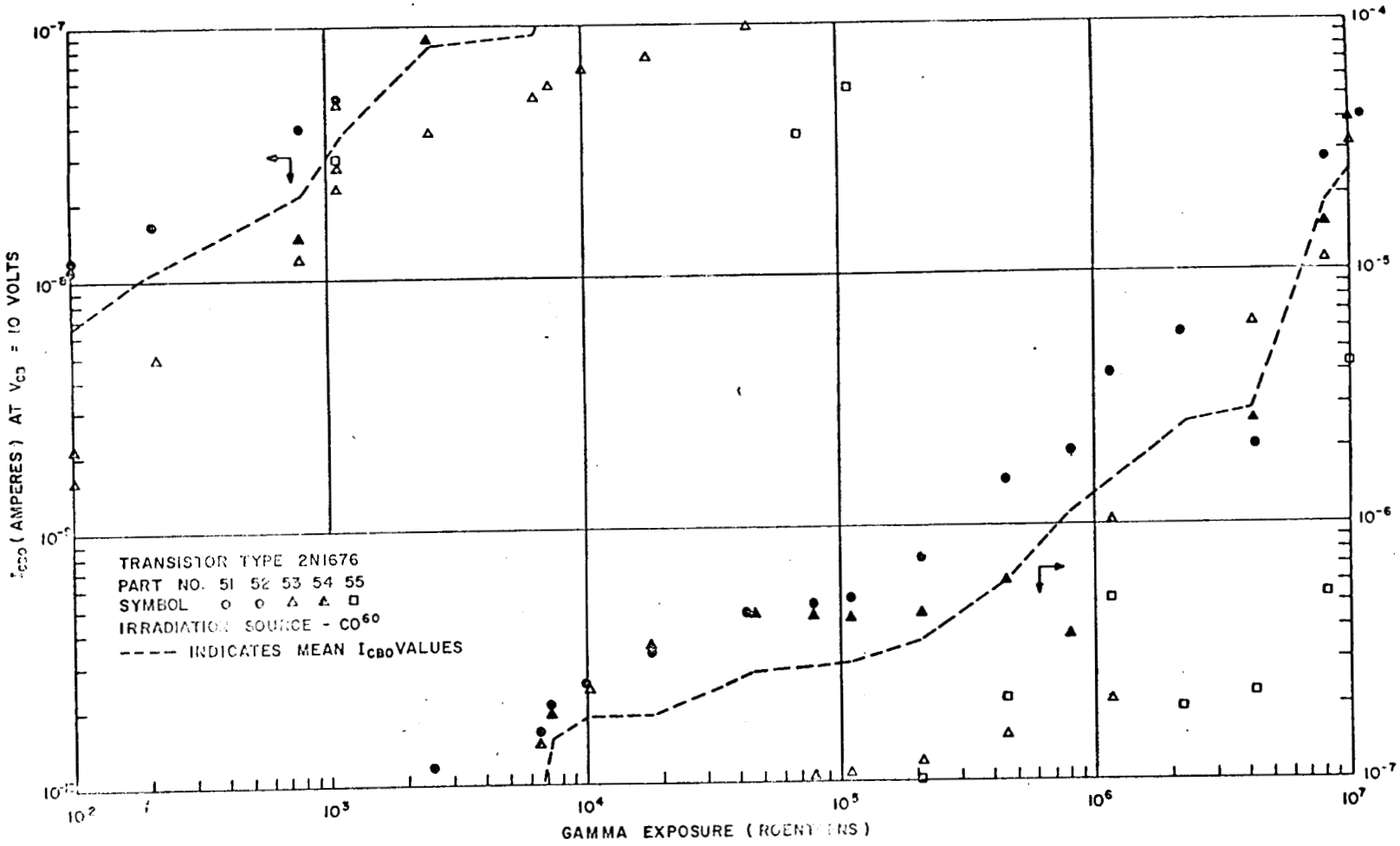

Figure 14. Radiation-Induced Damage (Transistor Type 2N1676)

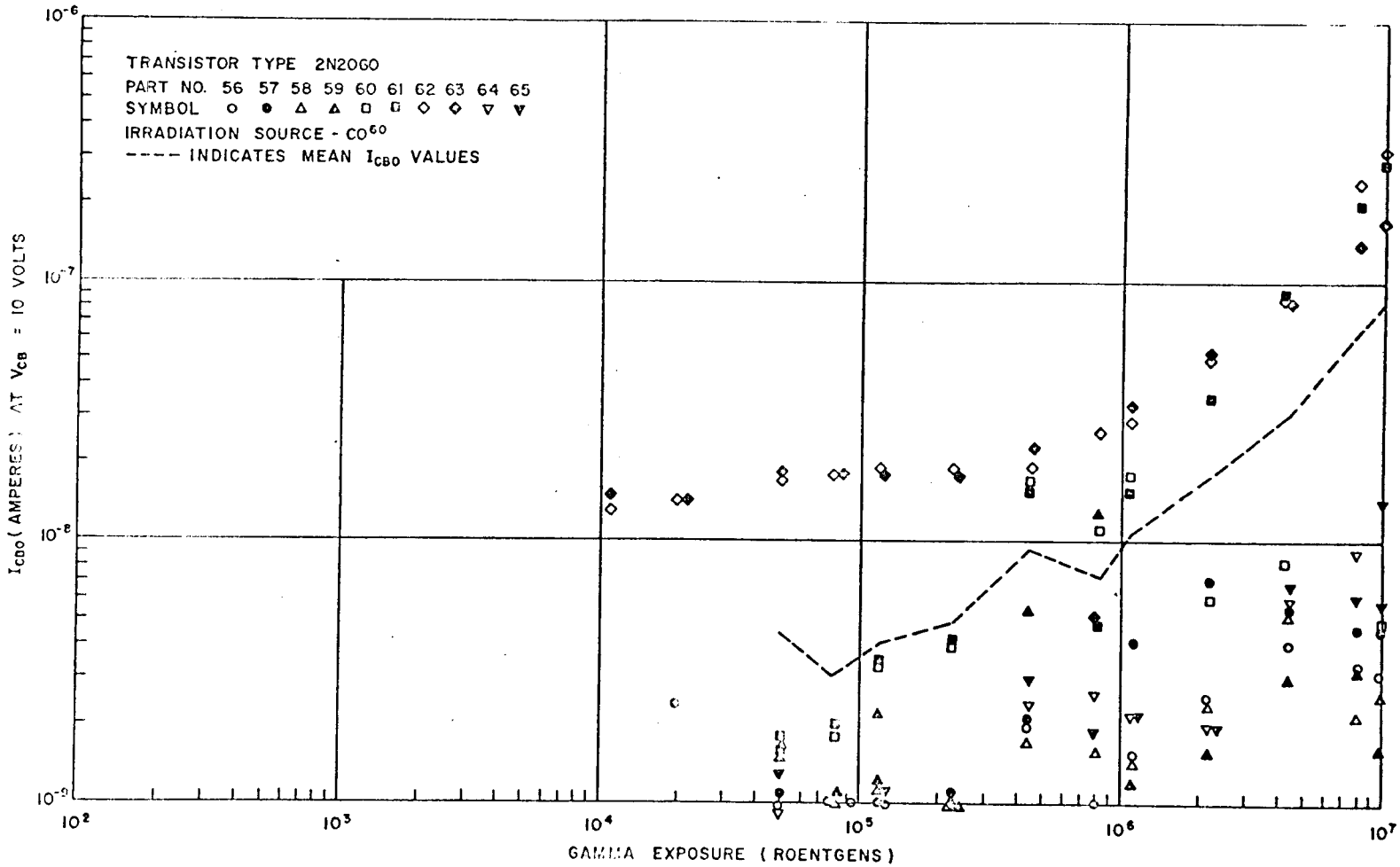

Figure 15-- Radiation Induced Damage (Transistor Type 2N2060)

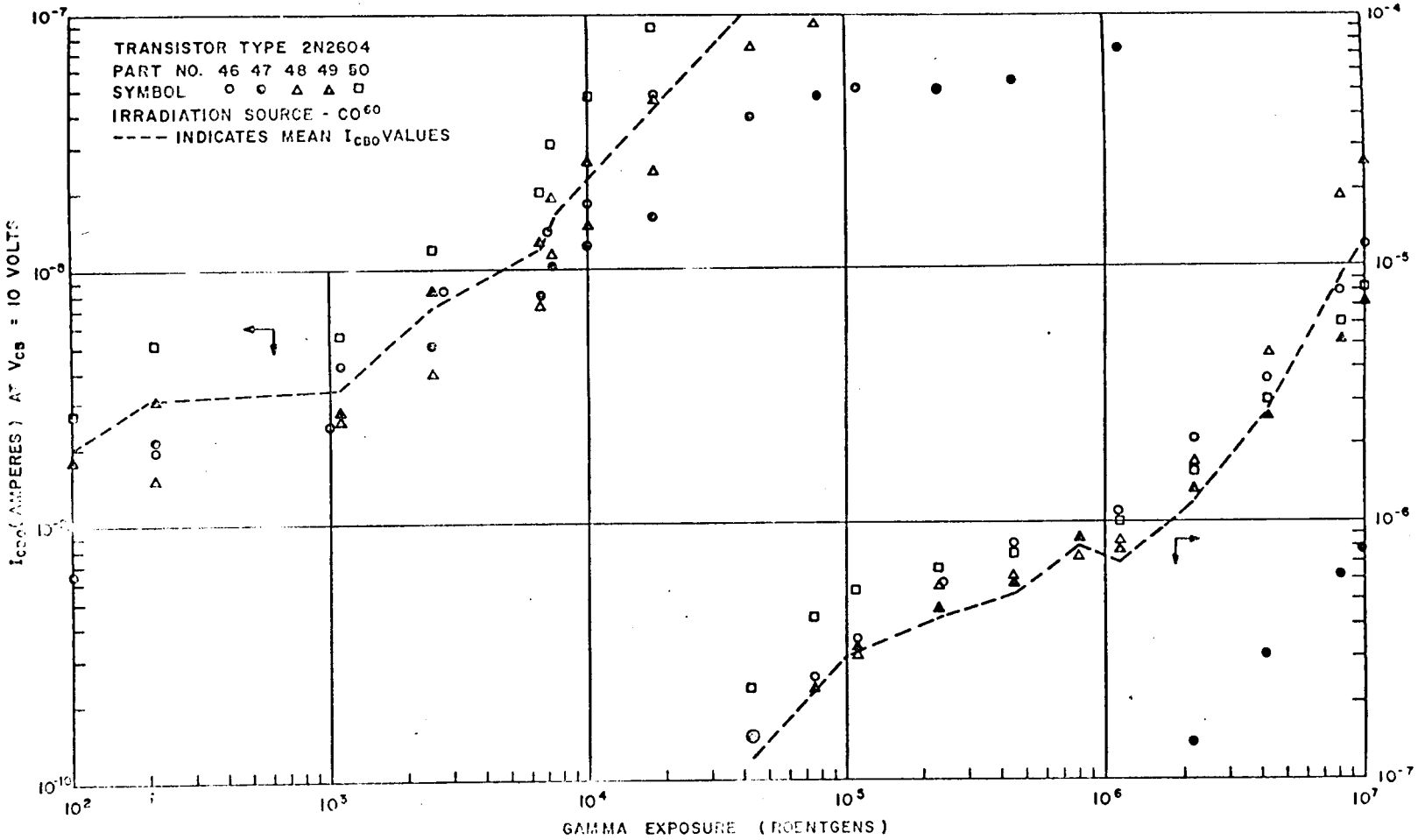

Figure 16-- Radiation-Induced Damage (Transistor Type 2N2604)

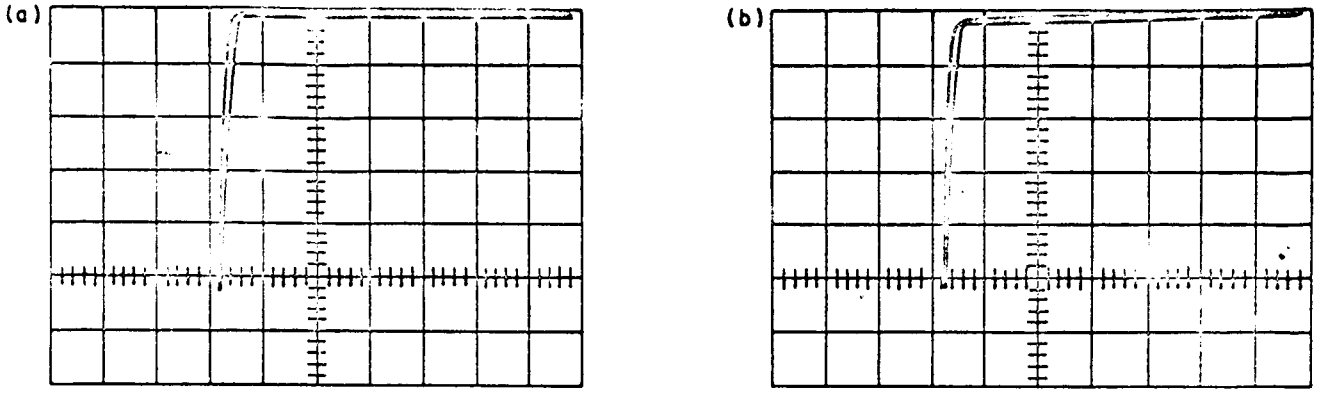

PRE-TEST
VERT 10μa/CM
HORIZ 20V/CM

POST-TEST
VERT 10μa/CM
HORIZ 20V/CM

REVERSE CHARACTERISTICS OF A TYPE IN914 DIODE

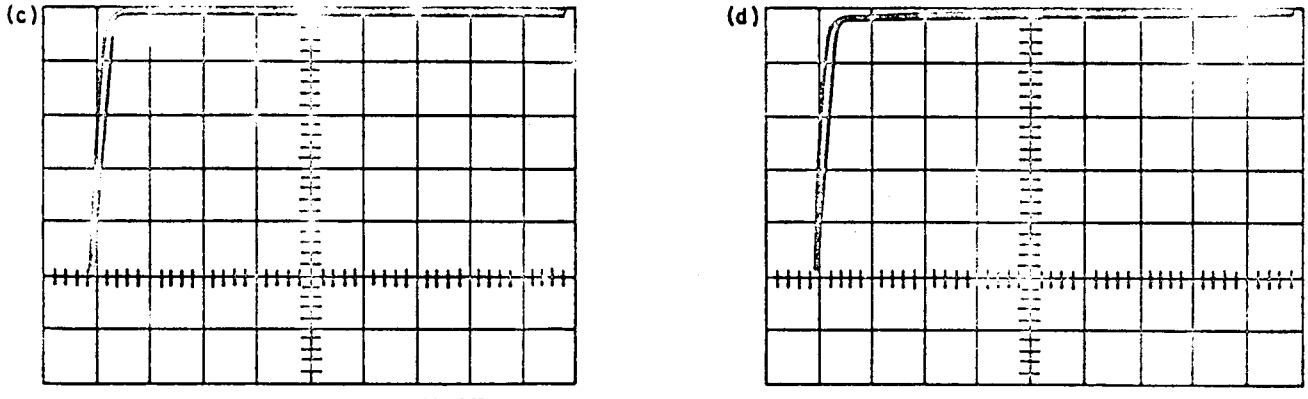

PRE-TEST
VERT 10μa/CM
HORIZ 10V/CM

POST-TEST
VERT 10μa/CM
HORIZ 10V/CM

REVERSE CHARACTERISTICS OF A TYPE MQ-1 DIODE UNAFFECTED BY RADIATION

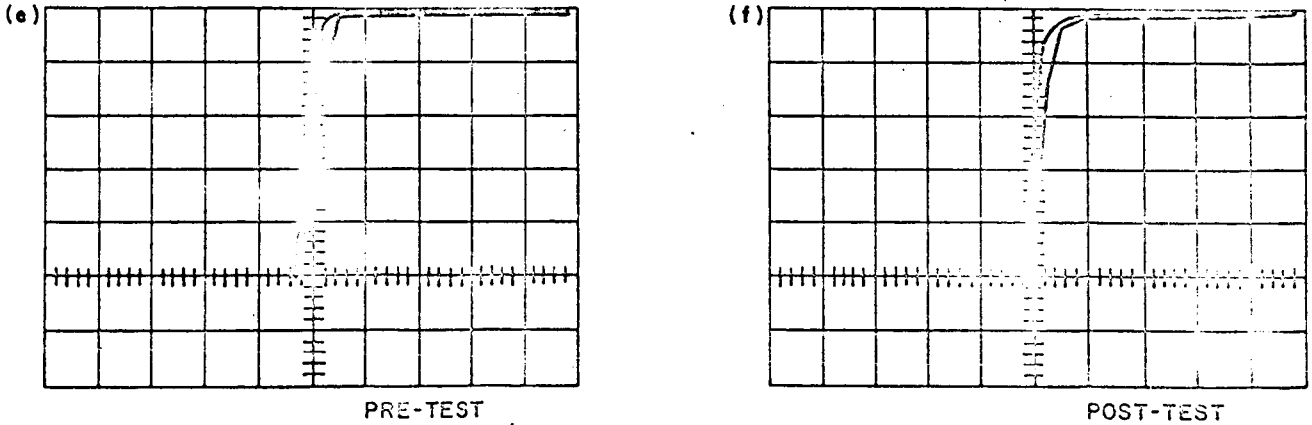

PRE-TEST
VERT 10μa/CM
HORIZ 20V/CM

POST-TEST
VERT 10μa/CM
HORIZ 20V/CM

REVERSE CHARACTERISTICS OF A TYPE MQ-1 DIODE EXHIBITING RADIATION DAMAGE

Figure 17--Reverse Characteristics of the 1N914 and MQ-1 Diodes

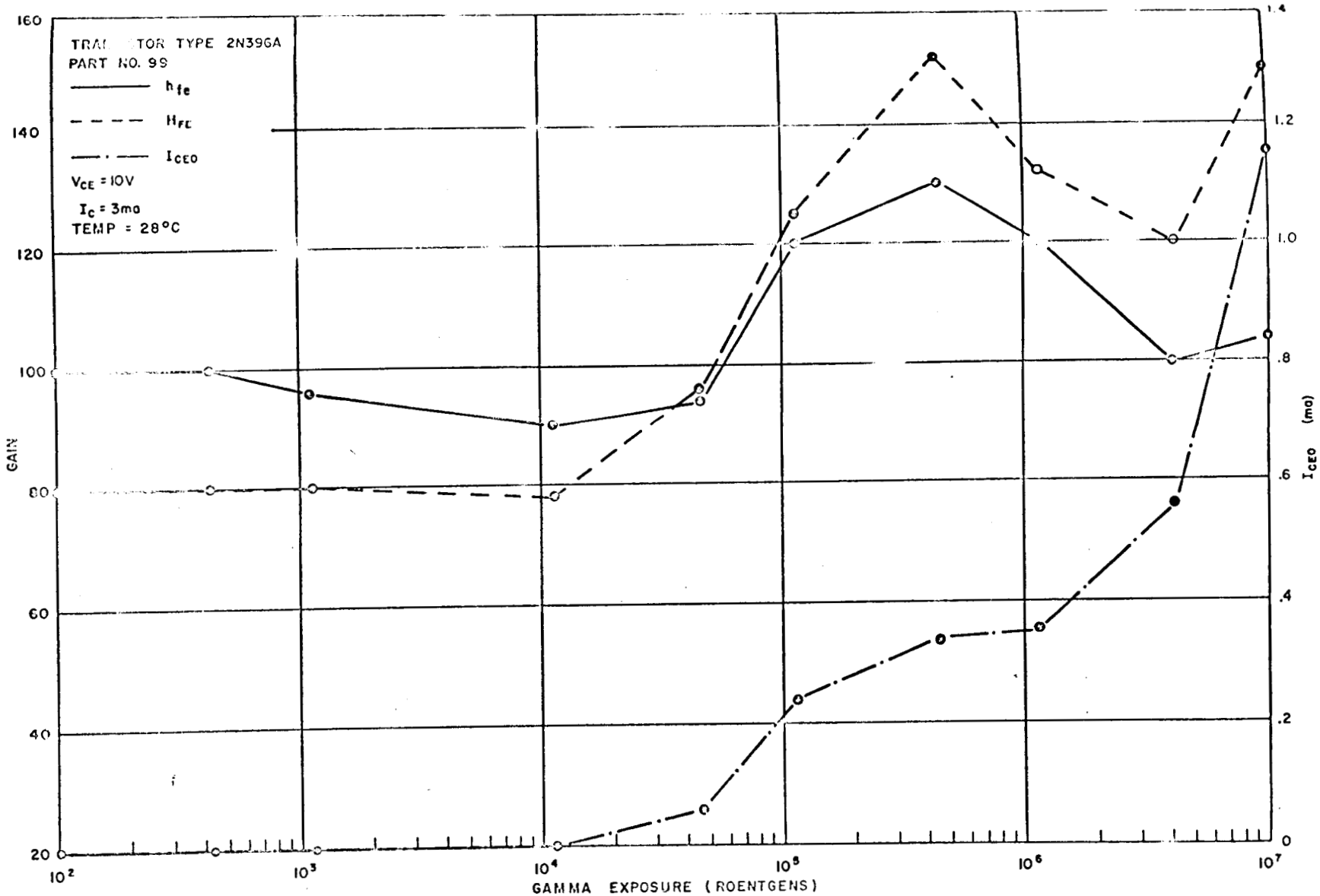

Figure 18--Radiation-Induced Gain Degradation (Transistor Type 2N396A)

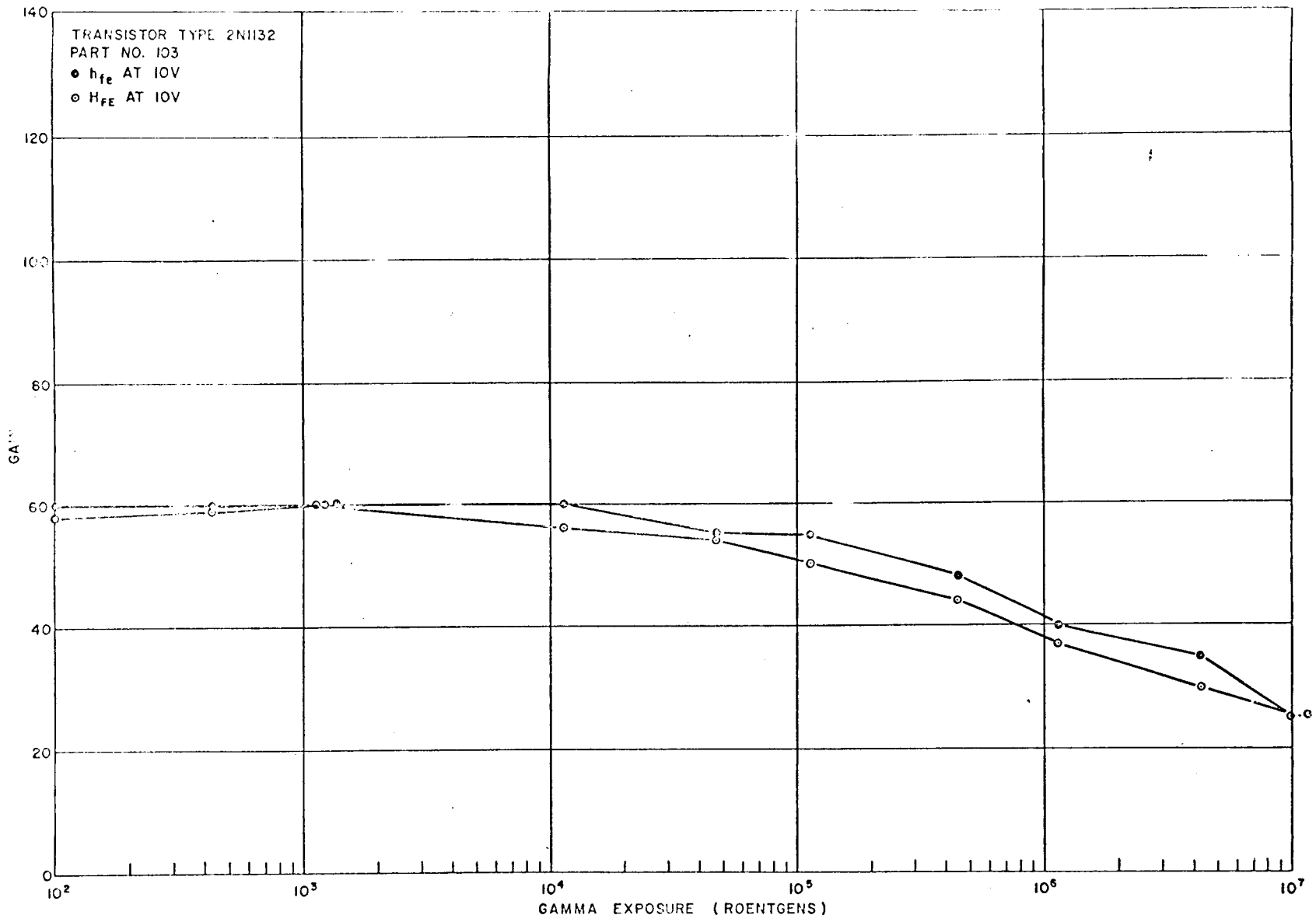

Figure 19 - Radiation-Induced Gain Degradation (Transistor Type 2N1132)

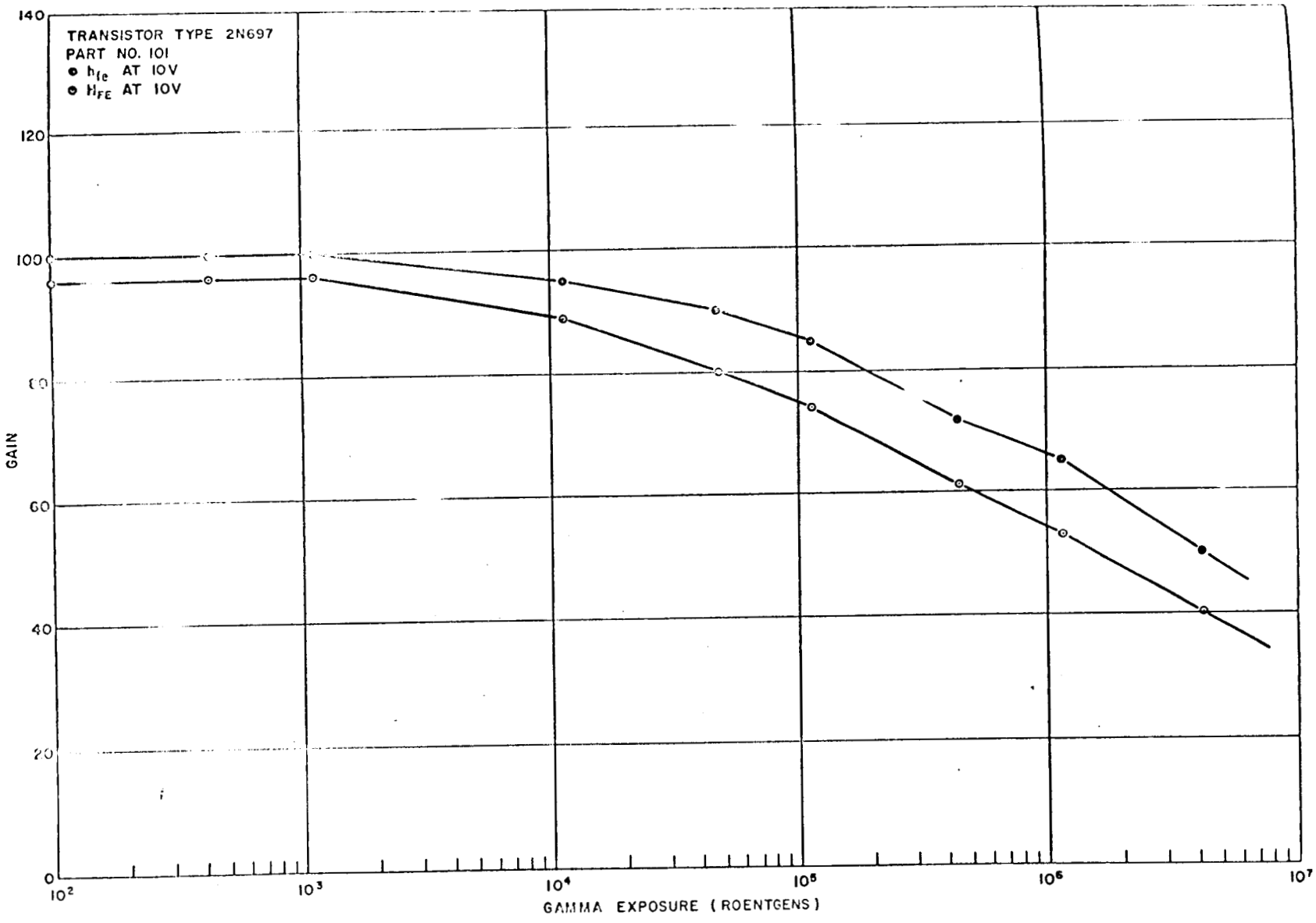

Figure 20 – Radiation-Induced Gain Degradation (Transistor Type 2N697)

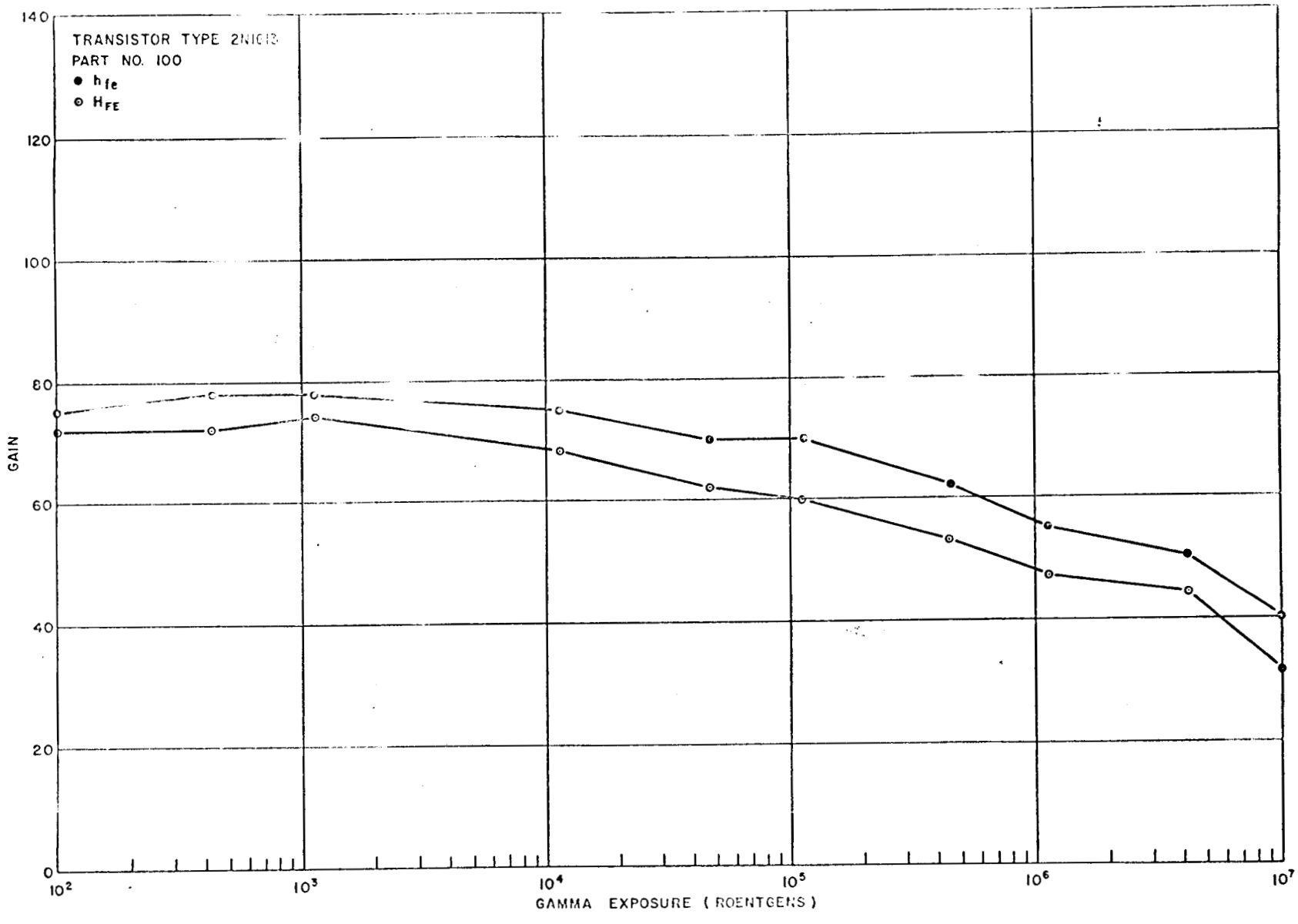

Figure 21-- Radiation-Induced Gain Degradation (Transistor Type 2N1613)

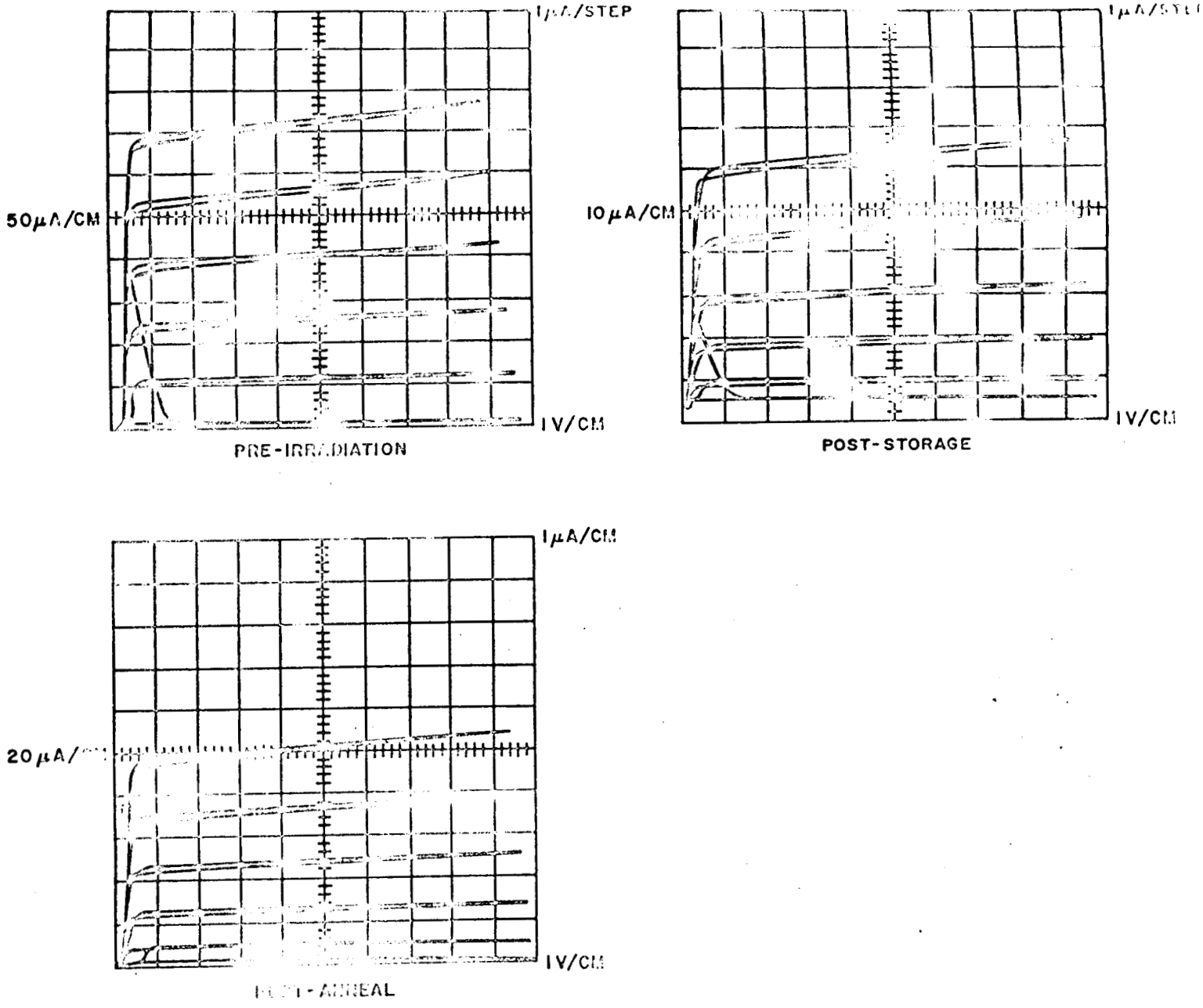

Figure 22--Radiation Damage to Collector Characteristics (Transistor Type 2N708)